



Non-destructively Differentiating the Roles of Creep, Wear and Oxidation in Long-Term In Vivo Exposed Polyethylene Cups

Giuseppe Pezzotti , Yasuhito Takahashi , Seita Takamatsu , Leonardo Puppulin , Takashi Nishii , Hidenobu Miki & Nobuhiko Sugano

To cite this article: Giuseppe Pezzotti , Yasuhito Takahashi , Seita Takamatsu , Leonardo Puppulin , Takashi Nishii , Hidenobu Miki & Nobuhiko Sugano (2011) Non-destructively Differentiating the Roles of Creep, Wear and Oxidation in Long-Term In Vivo Exposed Polyethylene Cups, Journal of Biomaterials Science, Polymer Edition, 22:16, 2165-2184, DOI: [10.1163/092050610X537129](https://doi.org/10.1163/092050610X537129)

To link to this article: <https://doi.org/10.1163/092050610X537129>



Published online: 02 Apr 2012.



Submit your article to this journal [↗](#)



Article views: 65



View related articles [↗](#)



Citing articles: 1 View citing articles [↗](#)

Non-destructively Differentiating the Roles of Creep, Wear and Oxidation in Long-Term *In Vivo* Exposed Polyethylene Cups

Giuseppe Pezzotti^{a,b,c,*}, Yasuhito Takahashi^a, Seita Takamatsu^a,
Leonardo Puppulin^a, Takashi Nishii^d, Hidenobu Miki^e and Nobuhiko Sugano^d

^a Ceramic Physics Laboratory & Research Institute for Nanoscience, Kyoto Institute of Technology, Sakyo-ku, Matsugasaki, 606-8585 Kyoto, Japan

^b The Center for Advanced Medical Engineering and Informatics, Osaka University, 2-2 Yamadaoka, Suita, Osaka 565-0871, Japan

^c Department of Orthopaedics, Orthopaedic Research Center, Loma Linda University, Loma Linda, CA 92354, USA

^d Department of Orthopaedic Medical Engineering, Osaka University Graduate School of Medicine, 2-2 Yamadaoka, Suita, Osaka 565-0854, Japan

^e Department of Orthopaedic Surgery, Osaka National Hospital, 2-1-14 Houenzaka, Chuo-ku, Osaka 540-0006, Japan

Received 26 February 2010; accepted 26 September 2010

Abstract

Wear of polyethylene acetabular cups in patients of total hip arthroplasty is routinely deduced from the penetration of the femoral head into the acetabular liner as observed in the radiographs. However, the linear penetration thus measured represents the cumulative contribution of two components, one due to wear, and the other due to creep or irreversible deformation of the polyethylene structure. The erroneous attribution to wear of the entire penetration displacement of the head in the cup might lead to misinterpretation of the actual performance of acetabular cups. The aim of this study was to quantify the head displacement components due to wear and to creep, as they occur *in vivo* in acetabular cups, and to relate them to the oxidation state of the material by means of advanced Raman spectroscopy procedures. Throughout the investigation, we compared the behaviors on the molecular scale of acetabular cups subjected to different sterilization methods (i.e., γ -irradiation and ethylene oxide treatment).

© Koninklijke Brill NV, Leiden, 2011

Keywords

UHMWPE, Raman spectroscopy, hip joint, acetabular cup, strain, oxidation

* To whom correspondence should be addressed. E-mail: pezzotti@chem.kit.ac.jp

1. Introduction

Creep and wear represent the two main degradation mechanisms found in various kinds of ultra-high-molecular-weight polyethylene (UHMWPE) acetabular cups that are responsible for their failure [1–3]. Creep refers to the permanent deformation that occurs under the effect of body weight and does not recover after load release, while wear involves both delamination and progressive peel-off of surface polyethylene flakes, resulting in the formation of minute and highly reactive debris. In the latter context, oxidation was found to play a detrimental role in triggering wear, since oxidized molecules might delaminate faster due to the embrittlement of the polymeric network [4]. In addition, the role of polymer molecular orientation and wear direction has also been comprehensively studied in UHMWPE acetabular components. In this context, the performance of the acetabular cups was shown to be highly dependent on the direction of shear [5]. In particular, greatly reduced wear rates have been reported for unidirectional, compared to multidirectional, articulation *in vitro*. This latter work has for the first time quantitatively shown that patient kinematics is an important factor affecting the wear and long-term biocompatibility of UHMWPE-bearing surfaces. The two degradation mechanisms of creep and wear might negatively interact and converge toward a cup-loosening effect, which mandatorily requires revision surgery. Unlike wear, creep is not accompanied by any irreversible mass loss from the material, but it involves packing and adjustment of polyethylene molecules in their reciprocal positions under pressure. Despite the different physical origin of these two main degradation mechanisms, from a phenomenological point of view, they both manifest themselves with a reduction in cup thickness, whose total extent is routinely measured both *in vivo* and on cup retrievals, and cumulatively recorded in clinical data.

Some of the early generations of polyethylene acetabular cups have been sterilized with ethylene oxide gas (EtO), while the majority of the conventional acetabular cups were sterilized with γ -radiation in air [5–8]. Sterilization with γ -irradiation causes cross-linking, which improves the wear-resistant property of polyethylene [9, 10]. However, such a procedure conducted in air increases the potential risk of oxidative degradation [5–8]. Therefore, most of the manufacturers changed to γ -sterilization in inert gas or gas plasma sterilization without radiation in the late 1990s because the shelf-time of polyethylene after gamma sterilization in air affects their oxidized state [7]. However, there was still a concern with residual free radicals which may oxidize polyethylene *in vivo*, although the impact of polyethylene oxidation on clinical results is dependent on the materials and design of polyethylene bearings [11–13]. Hence, polymer scientists and technologists have long studied methods to concurrently improve wear resistance, deformation/fracture resistance and oxidative stability of polyethylene materials by applying different manufacturing methods. In particular, treatments of UHMWPE have been the object of intensive research in order to maximize the creep resistance of the material without inducing tangible oxidation, embrittlement effects and wear enhancement [9, 14–17]. However, a lack of clarity can be found in comparing the intrinsic properties

of polyethylene materials and their actual performance when inserted in artificial hip joints. In examining the vast available literature, one may come across several aspects of the functional response of polyethylene types that are somewhat contradictory and represent a main concern for the aims of the present research, which are: (i) systematic measurements of the *in vitro* quasi-static tensile and compressive creep (bulk) properties of UHMWPE have been reported showing that crosslinking by γ -irradiation might significantly devalue the creep properties [18]. These negative data on the ‘intrinsic’ mechanical behavior are in contrast to some reports on hip simulator experiments [19] and, in general, to positive literature reporting that cross-linking reduces the head penetration rate *in vivo* and enhances the wear resistance of the polymer [20]. (ii) A significant effect was noted in a change of the pressure dependence of the wear rate on the γ -irradiation dose under inert atmosphere [21]. Thus, whether or not a sterilizing (or re-sterilizing) dose measurably enhances wear rate shall strongly depend on contact stresses. In this context, a milestone paper was written by Ingham and Fisher [22], who clarified the differences in biological responses to cross-linked and non-cross-linked UHMWPE, and showed that it is not the wear volume that determines the biological response to the debris, but the concentration of the wear volume comprised in the critical size range (0.2–0.8 μm). In their hip simulator study, Dowson and Jobbins [23] indicated that creep can account for an appreciable portion of the total penetration in 22 mm cups within the first few million cycles. However, a method for assessing the actual fraction of displacement due to creep in acetabular cups exposed *in vivo* is still lacking.

Important practical implications are involved with the complex time- and load-dependent *in vivo* results. The need to clarify several discrepancies in the role of intrinsic (e.g., the degrees of cross-linking and molecular alignment in the polyethylene structure [5, 24]) and extrinsic (e.g., patient kinematics and acetabular cup design [5, 25]) parameters affecting the performance of various polyethylene grades employed in hip arthroplasty calls for a better understanding of the relations between molecular structure and mechanical properties, including a substantial improvement in the methods of characterization.

In this paper, we have employed advanced techniques of confocal Raman spectroscopy, which we partly developed in previous studies [23, 26, 27] as a non-destructive tool for oxidation analysis and for differentiating, from the overall thickness decrease observed in acetabular cups exposed *in vivo*, the contributions respectively arising from creep and from wear. Additionally, we shall newly validate here (i.e., by means of case-by-case calibrations) a reliable and non-destructive method for measuring the residual strain profile along the cross-section of acetabular cups using spatially resolved Raman characterizations. Concurrently, we have also monitored the oxidation state of the material through a comparative analysis of Raman spectral regions representing vibrational twisting and wagging of the $-\text{CH}_2-$ bond of the polyethylene structure. A comparison is made here between two types of polyethylene cups, which were originally subjected to different sterilization procedures (i.e., EtO gas treatment and γ -irradiation) and exposed *in vivo* up to

25 years. We shall show that Raman measurements lead to more detailed analyses of retrieved acetabular liners as compared to conventional assessments by weight loss or liner penetration depth (radio-stereometric) analyses. This additional body of information should help shedding some light on the discrepancies found in the literature on the performance of liners made of different grades of polyethylene. The Raman method gives direct access to the vibrational response of the molecular structure of polyethylene and might provide a more rational guide, as compared to the available evaluation methods, for surgeons and technologists in quantitatively evaluating the true structural performance of polyethylene cups fabricated by different manufacturers.

2. Materials and Methods

2.1. Retrievals and Related Clinical Data

A total of 16 retrieved acetabular cups were obtained at the time of the respective hip arthroplasty revision surgeries, the majority of which were retrieved in a quite recent and narrow interval of time (Table 1). Fourteen cups were long-term (between 7.5 and 25.3 years) exposed and 2 cups short-term (between 0.7 and 1.8 years) exposed. Among the long-term exposed liners, 7 cups (from Kyocera) were made of the same grade of a conventional polyethylene material (GUR 412) and sterilized in EtO gas, while the remaining seven cups were from different makers (Table 1), but they were all cross-linked UHMWPE with surface irradiated by γ -rays. Note that also the cups sterilized in EtO were subjected to γ -irradiation in the range 25–40 kGy. The irradiation dose given to each investigated cup is also shown in Table 1. The available seven retrievals sterilized in EtO represented a quite homogeneous sampling, not only because they were made of the same material and belonged to the same type of implant, but also because they were all implanted by cemented hip arthroplasty against alumina-based materials, and were all retrieved for the same reason (aseptic loosening) after long-term exposure *in vivo* (i.e., in the interval between 16.8 and 25.3 years). Among the seven EtO-sterilized samples, six belonged to female patients aged between 49 and 74 years at the time of the revision surgery. All the γ -irradiated UHMWPE acetabular cups analyzed in this paper were from cementless hip arthroplasty; 5 of them were employed against CoCr femoral heads, while the remaining 4 cups were employed against alumina ceramic heads. Regarding to the age and sex of the patients, sampling for the γ -irradiated cups was statistically similar to that of the EtO-sterilized ones except for one short-term implanted sample that belonged to a rather young (32 years old) female patient. The two short-term (<2 years) *in vivo* exposed cups were both γ -irradiated (the shortest-term-exposed cup (0.7 years) was retrieved due to fracture/dislocation). Acetabular components revised for aseptic loosening had pre-revision radiographs, from which the head migration displacements were calculated. Such linear displacements were also measured in all the studied cups directly on the retrievals using a micrometer screw to obtain the cup thickness at the exact locations where spectro-

Table 1.
Overview of the cups tested in this study

| Sterilization | Sample | Age | Gender | Follow-up (years) | Manufacturer | Cup material | Total radiation dose (kGy) | External diameter (mm) | Δr (μm) | Δr_c (μm) | Femoral head | Cause of revision |
|---------------|--------|-----|--------|-------------------|--------------|--------------|----------------------------|------------------------|------------------------------|--------------------------------|---------------------|-------------------|
| Eto | 1 | 49 | Female | 25.3 | Kyocera | GUR412 | 25–40 | 42 | 5410 | 130 | 28 mm Alumina (AY7) | Cup loosening |
| | 2 | 60 | Female | 24.5 | Kyocera | GUR412 | 25–40 | 44 | 2500 | 59 | 28 mm Alumina (AY7) | Cup loosening |
| | 3 | 67 | Female | 22.2 | Kyocera | GUR412 | 25–40 | 42 | 3650 | 163 | 28 mm Alumina (AY7) | Cup loosening |
| | 4 | 51 | Female | 22.0 | Kyocera | GUR412 | 25–40 | 42 | 3760 | 262 | 28 mm Alumina (AY7) | Cup loosening |
| | 5 | 77 | Male | 21.1 | Kyocera | GUR412 | 25–40 | 46 | 3430 | 262 | 28 mm Alumina (AY7) | Cup loosening |
| | 6 | 52 | Female | 17.9 | Kyocera | GUR412 | 25–40 | 50 | 1700 | 129 | 28 mm Alumina (AY7) | Cup loosening |
| | 7 | 74 | Female | 16.8 | Kyocera | GUR412 | 25–40 | 44 | 3330 | 210 | 28 mm Alumina (AY7) | Cup loosening |

Table 1.
(Continued.)

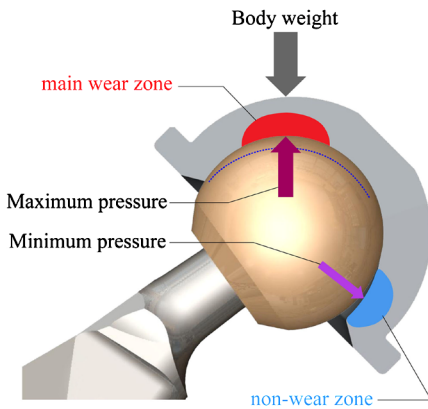
| Sterilization | Sample | Age | Gender | Follow-up (years) | Manufacturer | Cup material | Total radiation dose (kGy) | External diameter (mm) | Δr (μm) | Δr_c (μm) | Femoral head | Cause of revision |
|---------------|--------|-----|--------|-------------------|--------------|-------------------|----------------------------|------------------------|------------------------------|--------------------------------|--------------------------|----------------------|
| γ -Ray | 8 | 70 | Female | 20.8 | Zimmer | GUR415 | 25–40 | 48 | 1490 | 132 | 28 mm Alumina Biolox II | Cup loosening |
| | 9 | 64 | Female | 20.2 | Stryker | GUR415 | 25–40 | 44 | 4250 | 111 | | Cup loosening |
| | 10 | 65 | Female | 19.9 | Stryker | GUR415 | 25–40 | 48 | 3700 | 167 | | Cup loosening |
| | 11 | 48 | Female | 15.7 | Zimmer | GUR415 | 25–40 | 52 | 870 | 141 | 28 mm Alumina Biolox II | Stem breakage |
| | 12 | 73 | Female | 15.2 | Zimmer | GUR415 | 25–40 | 52 | 1600 | 228 | 28 mm Alumina Biolox II | Cup loosening |
| | 13 | 55 | Male | 11.1 | DePuy | GUR415 | 25–40 | 44 | 4260 | 307 | 22 mm CoCr | Cup loosening |
| | 14 | 60 | Female | 7.5 | Zimmer | GUR1050 | 90–110 | 46 | 2330 | 501 | 26 mm CoCr | Liner breakage |
| | 15 | 32 | Female | 1.8 | Stryker | GUR1050 Crossfire | 105 | 50 | 130 | 129 | 32 mm Alumina Biolox II® | Cup loosening |
| | 16 | 68 | Male | 0.7 | Stryker | GUR1050 Crossfire | 105 | 58 | 310 | 307 | 32 mm CoCr | Fracture dislocation |

scopic assessments were made in the main-wear zone. Linear displacements (*cf.*, Δt values in Table 1) were then obtained by subtracting the average thickness measured in the main-wear zone from the nominal thickness of an unused sample. Linear displacements in the main-wear zone and other salient details related to the clinical history of the retrievals are specified in Table 1. It should be emphasized that, from the viewpoint of the polyethylene performance, none of the 14 long-term-exposed retrievals examined in this study was defective, except for one of the γ -irradiated samples, which was retrieved for excessive liner wear (*cf.*, sample 14 in Table 1); in other words, the majority of the employed materials could be phenomenologically classified according to commonly expected trends for *in vivo* exposure as, for example, those predicted by parametric mathematical models based on the Archard's law [28] (e.g., thickness reduction according to a volumetric wear rate in the order of $5.8 \text{ mm}^3/\text{year}$ for a standard reference patient who is supposed to take an average of 1200 steps per day) or experimentally reported (e.g., about 15 years for UHMWPE cups vs CoCr heads [29], a lifetime eventually enhanced by about 25% in the case of using alumina femoral heads [30]).

2.2. Confocal Raman Analysis

Raman spectra were all collected at room temperature by means of a highly spectrally resolved triple-monochromator (T-64000, Jobin-Yvon/Horiba) equipped with a charge-coupled device (CCD) detector. Commercially available software (Lab-spec, Jobin-Yvon/Horiba) enabled the spectroscopic deconvolution of the Raman spectra. Spectra were fitted to Gaussian/Lorentzian mixed functions. For calibrating the dependence of selected Raman bands on applied strain under the Raman microprobe, a uniaxial compression jig was employed, as described in a previous report [27]. Briefly, we applied *in situ* a controlled state of strain to a calibration sample of each (initially unstrained) polyethylene type ($3 \times 3 \times 6 \text{ mm}$ in dimension), while monitoring the variation in width of a selected Raman band from the polyethylene spectrum. Samples for compression tests were obtained from the non-wear zone of the respective acetabular cups, in the neighborhood of the cup edge, as shown in Fig. 1a. These zones could be considered to be reasonably strain-free. For some types of cup (i.e., samples 14–16) of recent manufacture, also virgin samples were available. We repeated the compressive stress calibrations also on these virgin samples and found no appreciable difference with samples obtained from non-wear zones. For some In band width/strain calibrations, the Raman probe was located at approximately the center of the sample and, taking advantage of the high transparency of polyethylene, translated by $50 \mu\text{m}$ below the surface in order to minimize both shear strain and surface roughness effects. The obtained calibration plots of bandwidth vs applied strain, typically linear in nature up to high strain percents, were then used to analyze the unknown strain fields that remained stored in the retrievals. Assessments of oxidation index, OI, from the relative intensity of selected bands of the Raman spectrum of polyethylene have been fully validated in a previous paper by means of 'control' experiments using both Raman and infrared

(a)



(b)

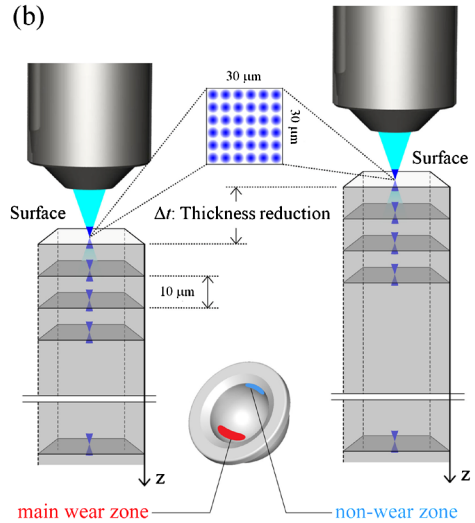


Figure 1. (a) Schematic showing the mechanics of acetabular cup deformation due to creep; (b) protocol for in-depth Raman mapping using a confocal probe configuration in both main-wear and non-wear zones. This figure is published in colour in the online edition of this journal, which can be accessed via <http://www.brill.nl/jbs>

spectroscopy exactly on the same samples [26]. In previous studies [26, 27], the equation linking relative Raman intensities to the oxidation parameter OI was found to be quite general for different types of polyethylene; therefore, no additional calibration experiments regarding the assessment of oxidation states were launched in the present study. All the Raman measurements on retrievals were made in a fully non-destructive way, without any sample manipulation, by focusing the confocal probe on both main-wear and non-wear zones of the studied acetabular cups. In the experimental analysis of acetabular cups, a confocal pinhole with an aperture diameter of 100 μm was placed in the optical circuit to exclude photons scattered from out-of-focus regions of the probe. Accordingly, only signals from a limited in-depth region close to the selected abscissa of the focal plane were brought to the detector and averaging effects due to the finite probe size, thus, could be minimized. A full description of the probe characteristics in polyethylene assessment has been given elsewhere [26]. The method for assessing Raman probe characteristics has been validated and it is widely used in other laboratories throughout the world [31, 32]. The confocal configuration of the probe adopted throughout the present experiments corresponded to a $\times 100$ objective lens; numerical objective aperture, confocal pinhole diameter and focal length of the objective lens were set as: $\text{NA} = 0.9$, $\Phi = 100 \mu\text{m}$ and $f = 11 \text{ mm}$, respectively. Figure 1 shows a draft of the *in vivo* location of the portions of the retrieved acetabular cups object of the Raman assessments and the related protocol for in-depth (non-destructive) evaluations by means of a Raman microprobe, respectively. Exploiting the high transparency of polyethylene, non-destructive in-depth scans allowed us to retrieve detailed sub-surface profiles of both strain and oxidation index along the entire thickness of the

retrieval cups. In the experimental practice, an automated sample stage with sub-micrometric step precision was employed, making it possible to record spectra at each depth with focusing below the sample surface, and to map spectra with lateral line scanning on the sample surface and sub-surface. Oxidation and strain profiles were collected with translating the focal plane along the in-depth (sub-surface) direction with micrometric resolution. Maps ($30 \times 30 \mu\text{m}$) were typically recorded at each location and depth and their spectra (900 spectra for each map) averaged to give the molecular vibrational modes of the polyethylene structure at each selected in-depth location. Measurements of sub-surface profile properties were eventually repeated at tens of locations in the main-wear zone, in order to obtain a statistical validation of the states of strain and oxidation for each of the retrievals investigated. The total number of collected Raman spectra on all the retrievals including both main-wear and non-wear zones was in the order of 1.5×10^6 for a total measurement time of about 4200 h.

3. Results

3.1. Validating the Assessment of Strain from Raman Spectra

In the molecular structure of polymers, an applied stress is directly translated into internal strain (in both bond angles and lengths) of the polymer backbone. Due to the anharmonicity of the atomic bonds, this circumstance brings about changes in the vibrational spectra, which can be probed by Raman spectroscopy. In general, a compressive strain causes a shift of Raman bands to higher wave-numbers whereas the reverse effect is observed in tension [33]. There is extensive literature on the dependence on strain of the Raman spectrum of polyethylene fibers and oriented films [34, 35]. However, unlike linear elastic materials, polyethylene shows a complex and strongly non-linear dependence of the Raman spectrum on strain. This circumstance makes it difficult a quantitative assessment of strain from band shift in the wide interval of plastic strains experienced by *in vivo* exposed acetabular cups. Fortunately in the case of polyethylene an additional phenomenon is observed: both C–C asymmetric stretching mode B_{1g} (1060 cm^{-1}) and symmetric stretching mode A_g (1127 cm^{-1}) bands split under strain into two components, which originate a broadening of the Raman bands. This has been interpreted as being due to a bimodal stress distribution of the C–C bonds in the material [33, 36–38]. Both tensile [39] and compressive [27] plastic strain have been directly measured in medical grades of UHMWPE by using a direct proportionality relationship between uniaxial strain and the increase in full-width at half maximum (FWHM) of a selected Raman band located at 1127 cm^{-1} (A_g mode). The rationale for bandwidth being a sensor of strain in the polymeric network resides in it reflecting the degree of disorder of the network and the degree of molecular orientation, which both are affected by strain. The increase of structural disorder under compressive strain is reflected in a broadening of the Raman band due to inter- and intra-lamellar slip processes. Additional phenomena leading to Raman band broadening have also been indicated,

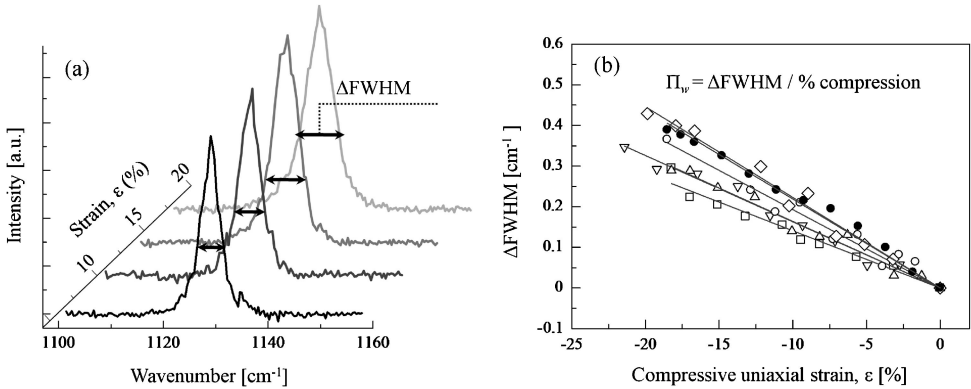


Figure 2. (a) Spectral band broadening as detected upon increasing the externally applied compressive strain for the EtO-sterilized polyethylene; (b) comparison among FWHM–strain calibration plots performed on all types of investigated polyethylene materials. The slope of the linear plots corresponds to: (●) -0.0219 (Kyocera GUR412); (◇) -0.0223 (Stryker GUR 415); (○) -0.0193 (Stryker GUR 1050 Crossfire); (△) -0.0164 (Zimmer GUR 415); (▽) -0.0163 (Zimmer GUR 1050); (□) -0.0141 (Depuy GUR 415).

as the beginning of crystallite fragmentation, fibril formation and chain disentanglement [40]. We selected broadening of the symmetric-stretching A_g band as a strain sensor because, unlike band spectral shift, such dependence is conspicuously linear up to quite large strain values (e.g., in the order of the tens of percents). However, despite such a straightforward relationship, a drawback of the Raman assessment of plastic strain by band-broadening method resides in its dependence on the individual polyethylene structure investigated; in other words, a lack of generality is found in the proportionality factor of the plot bandwidth vs strain, which necessarily requires preliminary case-by-case calibrations for each polyethylene grade investigated. In this study, strain calibration plots were obtained for all the investigated polyethylene materials, as shown in Fig. 2. Broadening of the symmetric C–C stretching band Raman (located at 1127 cm^{-1}) under compressive strain followed a clearly detectable (linear) trend for all the investigated materials (e.g., the sequence of spectra in Fig. 2a for the EtO-sterilized polyethylene), although the slopes of the respective plots were different as a result of the aforementioned structural dependence. In Fig. 2b calibration lines are explicitly given for all the investigated polyethylene structures. They were obtained according to the criterion of least-square fitting of the experimental data. A full description of the origin of the different slopes recorded in differently manufactured materials is beyond the scope of this paper. However, we can attribute to both a higher degree of molecular alignment and a lower structural disorder the lower (unstrained) C–C stretching bandwidth generally recorded in γ -irradiated as compared to EtO-sterilized materials. On the other hand, a higher slope found in the plots of FWHM vs strain is believed to capture the essence of a better shear-activated stress transfer mechanism, as already suggested by Tarantili *et al.* [33]. The plots of FWHM shown in Fig. 2b represent the basis for investigating the profiles of permanent strain stored

after long-term *in vivo* exposure in acetabular cups obtained from different manufacturers, which will be presented in the next section.

3.2. In-depth Profiles of Strain and Related Creep Deformation

Following the confocal procedures and the experimental outputs described in Sections 2.2 and 3.1, respectively, strain profiles that permanently remained stored in the main-wear and non-wear zones of retrieved cups could be measured and plotted as a function of depth along the sub-surface. These assessments required a choice of a standard (minimum) width for the symmetric C–C stretching band of polyethylene, for which the width of a band retrieved from the core of unused (and unloaded) acetabular cups was selected. In Fig. 3 strain profiles are shown, which were non-destructively collected at increasing probe depths in both main-wear and non-wear zones (Fig. 3a–g and 3h–n for EtO-sterilized and γ -irradiated long-term-exposed retrievals, respectively). In in Fig. 3, the number assigned to each sample corresponds to the sample number given in Table 1; it is, thus, increasing with decreasing exposure time *in vivo*. Each data point in the plots represents an average value retrieved over an area of $900 \mu\text{m}^2$ at each sub-surface depth. We plotted the strain profiles with placing a common origin for the plots on the internal surface of the acetabular cup at the time of measurement. For this reason, plots representing main-wear and non-wear zones correspond to the same probing depths but refer to different thicknesses of the liners. The thickness reductions, Δt , that cumulatively arose from both creep deformation and wear abrasion (i.e., as they piled up during the *in vivo* lifetime) are listed in Table 1. The Δt values could be retrieved because precise assessments of cup thickness in the main-wear zone were available from post-surgical measurements. It immediately appears that a rational trend in terms of the measured (overall) reduction of cup thickness indeed exists for the main wear zone as a function of service time *in vivo*; the longer the service time, the higher Δt . However, there are exceptions to this trend, especially in the γ -irradiated samples. This latter observation, which will be expanded in the discussion section, clearly reflects a long idiosyncratic difficulty in quantitatively assessing and rationalizing the actual *in vivo* performance of acetabular cups from different makers in terms of structural stability and rate of reduction of their initial thicknesses.

In the remainder of this paper, we shall take the creep profiles detected in the non-wear zone as representative of the residual state of strain in the main-wear zone before implantation, namely in the implants as-received from the maker. As a general trend, all the investigated cups were typically (residual) strain-free at the time of implantation. However, in comparing main-wear and non-wear zones in all samples, Raman experiments always revealed a significant increase in the amount of residual strain stored in polyethylene structures belonging to main-wear zones. The average uniaxial strain was typically in the order of 20% (in compression) for the EtO-treated implants (with only cup No. 5 in Table 1 showing a higher value (*cf.*, Fig. 3e). The average residual strain stored in the γ -irradiated samples after explantation was similar in magnitude but more scattered than that observed in the EtO

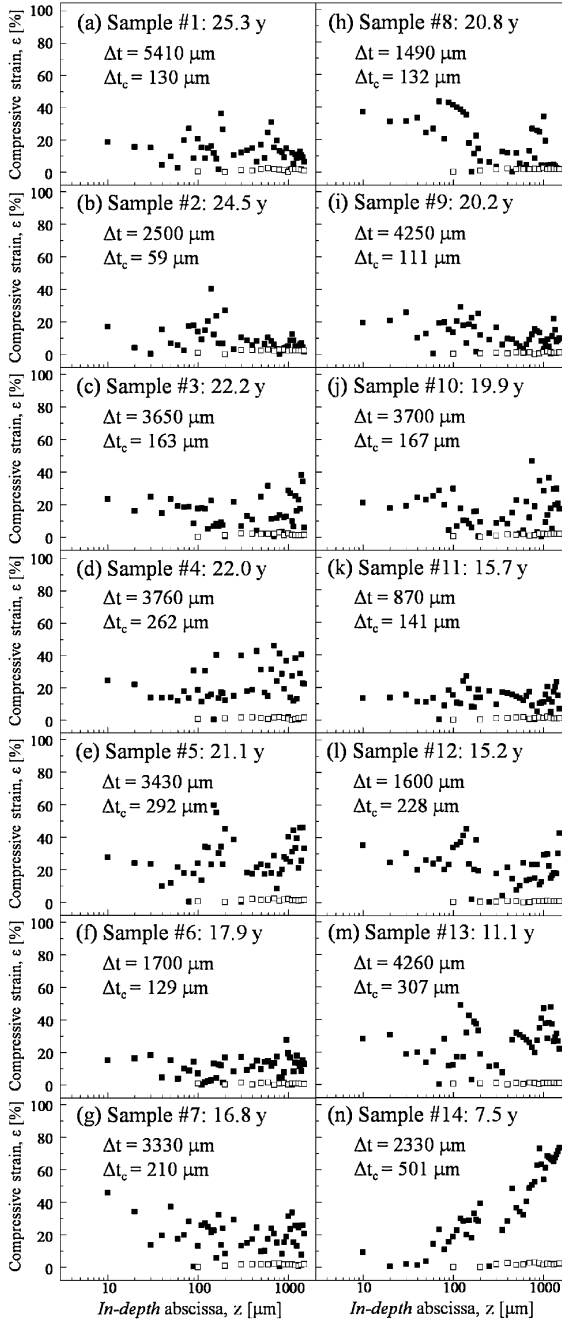


Figure 3. In-depth strain profiles collected on retrievals as listed in the respective insets and in Table 1 (open and close circles refer to non-wear and main wear zones, respectively).

treated implants. This data scatter should depend on the type of cross-linked polyethylene analyzed and on the homogeneity/accuracy of the adopted cross-linking

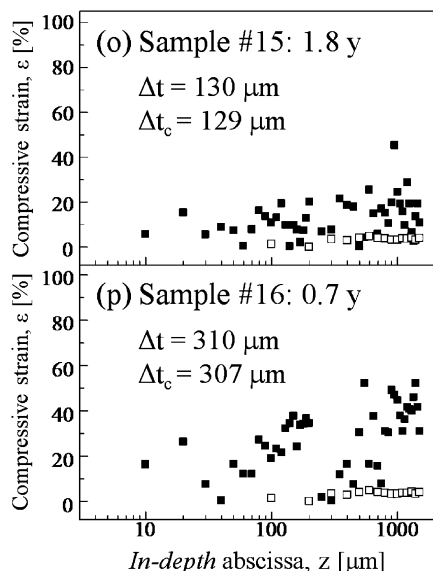


Figure 4. In-depth strain profiles collected in short-term retrievals sterilized with γ -rays (open and close symbols refer to non-wear and main wear zones, respectively).

process. Interestingly, strain maxima were not found in correspondence of the very surface of the material, but at depths of both several tens and several hundreds of μm . These results help visualizing the creep contribution to the *in vivo* penetration of femoral component into the polyethylene liners, and enable one quantifying the thickness reduction due to creep. In order to estimate the head-penetration component, Δt_c , due to creep at the time of the explantation of the liner, a numerical integration of the strain profile in the main-wear zone was performed over the entire thickness of the liner, as suggested in a previous report [27]. The results of this calculation are shown in Table 1. A general conclusion can be drawn from an examination of Δt_c data in comparison with the overall displacements, Δt : at the time of explantation, the creep contribution to the overall femoral head (linear) displacement onto the liner was always by far (i.e., from one to two orders of magnitude) lower than that due to wear (i.e., $\Delta t_w = \Delta t - \Delta t_c$). Figure 4 shows the residual strain profiles stored into two γ -irradiated samples that were implanted for only for 1.8 and 0.7 years, respectively (samples 15 and 16 in Table 1). The head-penetration component, Δt_c , due to creep at the time of the explantation of those short-term exposed liners was found to be comparable with that of the long-term implanted liners and with the total migration displacement of the head, Δt . These findings clearly show that the head displacement onto the liner is creep-dominated in the initial period (i.e., ≤ 0.7 years, according to the data presented here) of implantation and limited to a relatively small fraction of the overall linear migration after long-term *in vivo* exposure. From the available data, we can postulate that the head displacement rate into the liner for γ -irradiated samples was in average about

18 times faster in the first 1.8 years of implantation as compared to the remaining implantation period (i.e., between 1.8 and 28.8 years).

3.3. In-Depth Profiles of Oxidation and Their Relationship with Strain Profiles

The oxidation state of the polyethylene structure can be evaluated non-destructively from a comparative analysis of the Raman spectrum of the material in the two spectral regions of $-\text{CH}_2-$ twisting vibration (at around 1300 cm^{-1}) and of $-\text{CH}_2-$ bond wagging (between 1350 and 1500 cm^{-1}). In particular, the Raman intensities of the bands located at 1414 cm^{-1} (characteristic of the orthorhombic crystal polymorph) and at 1293 cm^{-1} (representing the overall degree of crystallinity of the polyethylene structure) are used for this evaluation. Since the Raman method for oxidation assessments in polyethylene has been previously validated in comparison with infrared spectroscopy data [26], we shall present hereafter directly the outputs of oxidation assessments in the studied samples without further validation of the assessment method. Figure 5 shows the OI profiles non-destructively collected at increasing depths in both main-wear and non-wear zones for EtO-sterilized (Fig. 5a–g) and γ -irradiated (Fig. 5h–n) retrievals, respectively. Average OI values in the main- and non-wear zones (OI_m and OI_n , respectively) are also explicitly shown in each plot. As in the case of creep strain profiles, the order of the plot is dictated by the decrease of their elapsing time of exposure *in vivo*, according to Table 1. It should be noted that nearly all the long-term implants examined in this study matched the lifetime expectations given by the respective makers. Nevertheless, from a comparison among the 14 profiles shown in Fig. 5, three striking features could be noticed: (i) the OI values measured in the non-wear zones were in general much more pronounced in γ -irradiated samples than in the EtO-sterilized ones; (ii) for both types of implants, the overall amount of oxidation did not significantly increase after even very long *in vivo* exposures (the present data were in reasonable agreement with oxidation profiles measured by other techniques on explanted cups made of γ -irradiated polyethylene materials [41]); and, (iii) the OI values in the main-wear zones were slightly lower for EtO-sterilized retrievals as compared to the γ -irradiated ones.

Maxima of OI were found in the far depth of the cup thickness, as widely reported and explained in terms of delamination in artificial joints [42–45]. However, the data shown here clarify that in the immediate sub-surface of the retrieved cups another OI maximum can be found at locations roughly coincident with the depths at which maxima were observed in the profiles of compressive strain. Complete plots of in-depth OI profiles (i.e., containing two OI maxima) have also been previously published and discussed [27]. We show here a more complete set of data, which should help, building upon previous findings, to better confirm the effect of creep on oxidation.

A comparison can again be made with the oxidation profiles observed in the short-term exposed acetabular cups (samples 15 and 16 in Table 1). The oxidation profiles measured by Raman in the main-wear and non-wear zones for these

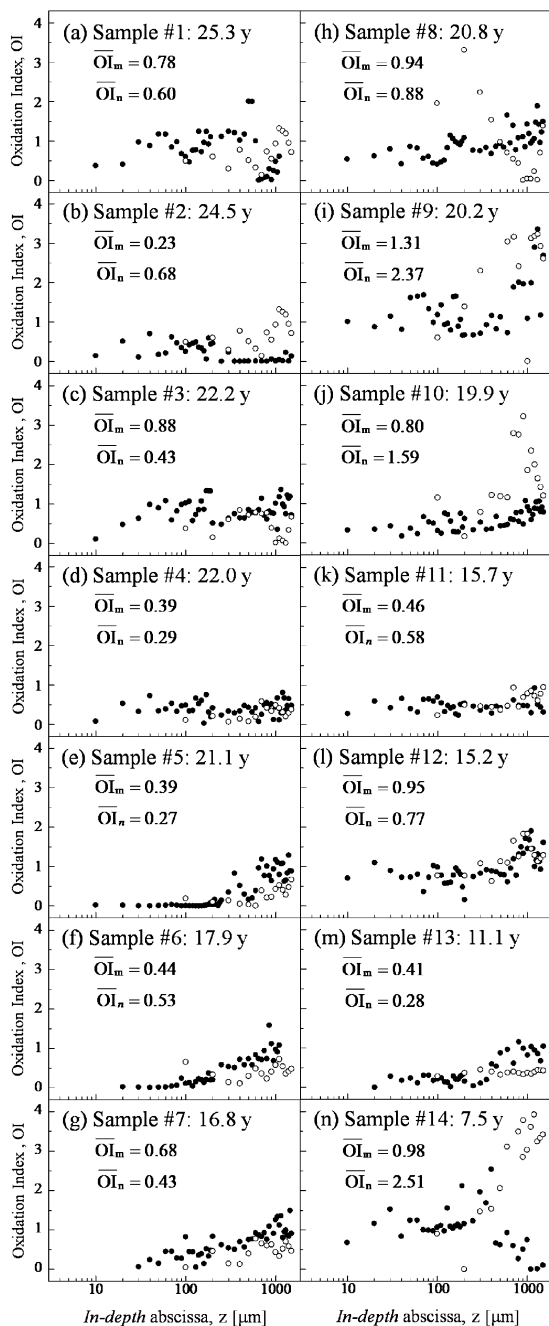


Figure 5. In-depth oxidation profiles collected on retrievals as listed in the respective insets and in Table 1 (open and close circles refer to non-wear and main wear zones, respectively).

latter two samples are shown in Fig. 6. Profiles of OI were similar in main-wear and non-wear zones for both samples and the maximum OI value was similar to

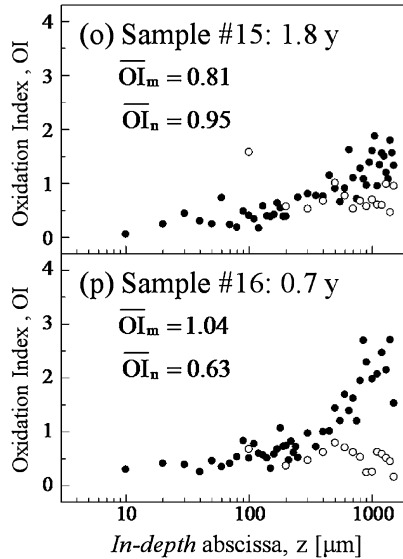


Figure 6. In-depth oxidation profiles collected in short-term retrievals sterilized by γ -rays (open and close symbols refer to non-wear and main wear zones, respectively).

those detected in the main-wear zones of long-term-exposed γ -irradiated cups, although the profile morphology as a function of in-depth abscissa was different (i.e., monotonically increasing and not showing intermediate maxima).

An attempt to interpret and rationalize the different sets of Raman data will be made in the next section based on a process of strain-assisted oxidation in acetabular polyethylene cups and on the role of initial oxidation state of the liner.

4. Discussion

According to the new experimental information provided in the above results section by means of highly spatially resolved Raman spectroscopy, the occurrence of severe oxidation paths just below the exposed surface of *in vivo* exposed polyethylene components calls for a re-consideration of the kinetics of the oxidation processes as compared to previous literature, and in particular of the peculiar role of compressive strain on the oxidation process. In a recent randomized clinical study, Glyn-Jones *et al.* [46] have analyzed the creep and wear behavior of highly cross-linked and standard polyethylene liners over a short-term implantation time (i.e., 3 years) using radio-stereometric analysis. These researchers showed that penetration of the femoral head onto the liner was creep-dominated in the first 6 months of implantation; while, after one year, the creep component of the overall migration displacement saturated and virtually all the additional penetration was due to wear. The conclusion of this study was that highly cross-linked polyethylene experienced a 60% lower rate of wear than standard polyethylene, from which it was extrapolated that cross-linked polyethylene will probably perform better in the long term. The outputs of our Raman studies on retrieved polyethylene liners can be used to

validate those conclusions, although we do not have in our present data the ‘deterministic’ resolution in terms of exposure time for rigorously distinguishing between our 0.7 or 1.8 years implanted samples and the samples implanted up to 3 years analyzed by Glyn-Jones *et al.* [46]. We have indeed found that the creep component (Δt_c) was the dominant contribution to the overall migration displacement of the femoral head in short-term *in vivo* exposed retrievals, but it represented a minor part of the overall displacement Δt measured at the time of explantation. On the other hand, the wear component (Δt_w) represented by far the dominant fraction of the overall head displacement Δt in long-term-exposed liners at the time of explantation. The unavailability of short-term retrievals for EtO-sterilized liners does not allow us a direct comparison to assess the contribution of the initial creep displacement on the overall linear migration of the femoral heads measured at the time of revision surgery. However, the amount of residual strain stored in the EtO-sterilized liners showed no statistical difference in comparison to γ -sterilized liners at the time of revision surgery (the exceptional strains recorded in sample 5 can be attributed to a larger clearance in this implant, as suggested by finite element simulation studies by Bewill *et al.* [47]). As we anticipated in the introduction, increased radiation to achieve a high level of cross-linking, might reduce some of the intrinsic mechanical properties of γ -irradiated materials [18], including elastic modulus and yield strength, thus increasing creep displacements. However, our study did not reveal a substantial difference between creep displacements measured in EtO- and γ -sterilized liners. In other words, the present spectroscopic data validate the numerical and experimental analyses of contact stress recently published by Plank *et al.* [48], showing that the use of relatively large femoral heads can confine contact stresses below a threshold value for structural yielding, even in highly irradiated (i.e., with intrinsically lower deformation resistance) polyethylene liners.

In vivo oxidation of polyethylene occurs in the presence of unstabilized radicals within the polymer and molecular oxygen uptake from body fluids and tissues [49]. The results of previous investigations have suggested that an OI > 3 is associated with a ‘critical’ step in the loss in mechanical properties and a propensity for fatigue damage *in vivo* [50]. Accordingly, OI < 1 can be interpreted as insignificant levels of oxidation and would not affect the ultimate mechanical performance of polyethylene. Furthermore, a lack of correlation found in the literature between oxidation state and clinical performance also suggests that a level of oxidation OI > 3 may be necessary to compromise the mechanical performance of polyethylene. From this latter point of view, none of the OI profiles reaches, at the time of explantation and for both types of liner investigated, a level of oxidation for which a substantial degradation of mechanical properties can be suspected. On the other hand, it is remarkable that 4 of the 8 investigated γ -irradiated samples were oxidized to OI = 3 or even slightly larger in their non-wear zones, thus suggesting the two following possibilities: (i) femoral heads might have blocked oxygen-containing fluid in the weight-bearing zone, thus promoting oxidation even

in the absence of strain fields; or (ii) the acetabular cups might have been already partly oxidized at the time of primary surgery.

Since the short-term exposed samples could have been already faulted samples at the time of implantation (i.e., not necessarily due to a manufacturing error but eventually to an inappropriate conservation on shelves), a comparison of creep and oxidation profiles in main-wear and non-wear zones of short-term and long-term γ -irradiated samples unfortunately cannot be used to substantiate the outcomes of our previous study [27], showing that creep occurs before oxidation in normally performing (i.e., not faulted) liners. However, additional information is obtained here on the role of excessive initial oxidation on the wear performance. Near-surface oxidation is known to contribute accelerating wear mechanisms in polyethylene acetabular cups during service [4]. Buchanan *et al.* [51] reported that accelerated aging of ultra high molecular weight polyethylene in pressurized oxygen results in peaks of polymer density and degree of oxidation up to 500 μm below the polymer surface. Shelf and *in vivo* aging was also found leading to density increases (i.e., mainly arising from changes in crystallinity) below the sample surface. Formation of microscopic cracks may occur *in vivo* in regions of maximum crystallinity [52], assisted by the presence of high sub-surface (contact) strain gradients. In highly oxidized zones, the microscopic elongation needed to locally break the polyethylene structure decreases [53], thus wear is accelerated. We found here that at least four out of the eight investigated retrievals of γ -irradiated liners could have experienced an $\text{OI} \geq 3$ at the time of implantation in the patient. These liners, all retrieved because of aseptic loosening, showed abnormal head migration displacements onto the liner, namely which degraded the structural performance of these liners below the standard performance of liners made of a less advanced EtO-sterilized polyethylene.

5. Conclusion

Quantitative methods of Raman spectroscopy have been applied to describe and to compare the magnitude of residual creep strain and the oxidation index in acetabular liners made of different polyethylene grades. Exploiting the main advantage of a non-contact and spatially resolved (confocal) probe enabled us to assess the correct in-depth morphology of strain and oxidation profiles stored in both main-wear and non-wear zones of liners sterilized with EtO gas or γ -irradiation. The main outcomes of our investigation can be summarized as follows:

- (i) Creep contributes the dominant portion to the overall migration displacement of the femoral head in short-term *in vivo* exposed retrievals, but it represents only a minor part of the overall displacement measured at the time of explantation.
- (ii) Independent of sterilization procedure, the wear component represents by far the dominant fraction of the overall head displacement in long-term-exposed liners at the time of explantation.

- (iii) The use of relatively large femoral heads confines the magnitude of contact stresses below a threshold value for structural yielding in highly irradiated polyethylene liners, thus making their creep performance comparable to that of EtO-sterilized liners.
- (iv) A large fraction (50%) of the investigated γ -irradiated samples were heavily oxidized (OI 3) in their non-wear zones and presumably also at the time of primary surgery. Such faulted components experienced wear rates comparable or even below those of standard EtO-sterilized liners.

The Raman spectroscopic method is proved here to provide new information on the molecular scale that is unavailable by previously established analyses (e.g., radio-stereometry). Screening retrievals by a confocal Raman probe have the potential to become a routine procedure in rationalizing the effect of residual strain and oxidation on the lifetime of polyethylene bearing surfaces.

References

1. B. Wroblewski, *J. Bone Joint Surg. Am.* **67**, 757 (1985).
2. M. D. McDonald and R. D. Bloebaum, *J. Biomed. Mater. Res.* **29**, 1 (1995).
3. J. Huber, A. Walter, W. Plitz and H. J. Refior, *Biomed. Tech. Berl.* **40**, 88 (1995).
4. P. Taddei, S. Affatato, C. Fagnano, B. Bordini, A. Tinti and A. Toni, *J. Mol. Struct.* **613**, 121 (2002).
5. S. M. Davey, J. F. Orr, F. J. Buchanan, J. R. Nixon and D. Bennett, *Biomaterials* **26**, 4993 (2005).
6. D. A. Fisher, *J. Arthroplast.* **14**, 925 (1999).
7. S. M. Kurtz, C. M. Rimnac, W. J. Hozack, J. Turner, M. Marcolongo, V. M. Goldberg, M. J. Kraay and A. A. Edidin, *J. Bone Joint Surg. Am.* **87**, 815 (2005).
8. P. D. Kiely, J. A. Harty and J. P. McElwain, *Acta Orthop. Belg.* **71**, 429 (2005).
9. M. Goldman, R. Gronsky, R. Ranganathan and L. Pruitt, *Polymer* **37**, 2909 (1996).
10. C. Heisel, M. Silva, M. A. dela Rosa and T. P. Schmalzried, *J. Bone Joint Surg. Am.* **86**, 748 (2004).
11. P. Eyerer and Y. C. Ke, *J. Biomed. Mater. Res.* **18**, 1137 (1984).
12. E. Gomez-Barrena, S. Li, B. S. Furman, B. A. Masri, T. M. Wright and E. A. Salvati, *Clin. Orthop. Relat. Res.* **352**, 105 (1998).
13. S. Stea, B. Antonietti, F. Baruffaldi, M. Visentin, B. Bordini, A. Sudanese and A. Toni, *Int. Orthop.* **30**, 35 (2006).
14. S. Williams, G. Isaac, P. Porter, J. Fisher and J. Older, *Clin. Orthop. Relat. Res.* **466**, 366 (2008).
15. S. Affatato, G. Bersaglia, M. Rocchi, P. Taddei, C. Fagnano and A. Toni, *Biomaterials* **26**, 3259 (2005).
16. H. A. McKellop, P. Campbell, S. H. Park, T. P. Schmalzried, P. Grigoris, H. C. Amstutz and A. Sarmiento, *Clin. Orthop.* **311**, 3 (1995).
17. J. Kabo, S. Gebhard, G. Loren and H. Amstutz, *J. Bone Joint Surg. Br.* **75**, 254 (1993).
18. G. Lewis and M. Carroll, *Biomed. Mater. Eng.* **11**, 167 (2001).
19. A. L. Galvin, E. Ingham, M. H. Stone and J. Fisher, *J. Bone Joint Surg. Br.* **88**, 236 (2006).
20. G. Digas, J. Thanner, B. Nivbrant, S. Rohrl, H. Strom and J. Kärrholm, *Acta Orthop. Scand.* **74**, 531 (2003).
21. R. M. Rose, E. V. Goldfarb, E. Ellis and A. N. Crugnola, *J. Orthop. Res.* **2**, 393 (2005).
22. E. Ingham and J. Fisher, *Proc. Inst. Mech. Eng. Part H* **214**, 2041 (2000).

23. D. Dowson and B. Jobbins, *Eng. Med.* **17**, 111 (1988).
24. Y. Takahashi, L. Puppulin, W. Zhu and G. Pezzotti, *Acta Biomater.* **6**, 3583 (2010).
25. W. G. Hamilton, R. H. Hopper Jr., S. D. Ginn, N. P. Hammell, C. A. Engh Jr. and C. A. Engh, *J. Arthropl.* **20** (Suppl. 3), 63 (2005).
26. G. Pezzotti, T. Kumakura, K. Yamada, T. Tateiwa, L. Puppulin, W. Zhu and K. Yamamoto, *J. Biomed. Opt.* **12**, 014011 (2007).
27. T. Kumakura, L. Puppulin, K. Yamamoto, Y. Takahashi and G. Pezzotti, *J. Biomater. Sci. Polymer Edn* **20**, 1809 (2009).
28. R. Pietrabissa, M. Raimondi and E. Di Martino, *Med. Eng. Phys.* **20**, 199 (1998).
29. A. A. Edidin, C. M. Rinnac, V. M. Goldberg and S. M. Kurtz, *Wear* **250**, 152 (2001).
30. A. Galvin, C. Brockett, S. Williams, P. Hatto, A. Burton, G. Isaac, M. Stone, E. Ingham and J. Fisher, *Proc. Inst. Mech. Eng. Part H* **222**, 0954-4119 (2008).
31. D. M. Lipkin and D. R. Clarke, *J. Appl. Phys.* **77**, 1855 (1995).
32. A. Atkinson and S. C. Jain, *J. Raman Spectrosc.* **30**, 885 (1999).
33. P. A. Tarantili, A. G. Andreopoulos and C. Galiotis, *Macromolecules* **31**, 6964 (1998).
34. J. A. H. M. Moonen, W. A. C. Roovers, R. J. Meier and B. J. Kip, *J. Polym. Sci. Part B: Polym. Phys.* **30**, 361 (1992).
35. R. P. Wool, R. S. Bretzlaff, B. Y. Li, C. H. Wang and R. H. Boyd, *J. Polym. Sci. Part B: Polym. Phys.* **24**, 1039 (1986).
36. K. Tashiro, G. Wu and M. Kobayashi, *Polymer* **29**, 1768 (1988).
37. W. F. Wong and R. J. Young, *J. Mater. Sci.* **29**, 510 (1994).
38. F. Rull, A. C. Prieto, J. M. Casado, F. Sobron and H. G. M. Edwards, *J. Raman Spectrosc.* **24**, 545 (1993).
39. M. Kyomoto, Y. Miwa and G. Pezzotti, *J. Biomater. Sci. Polymer Edn* **18**, 165 (2007).
40. R. Hiss, S. Hobeika, C. Lynn and G. Strobl, *Macromolecules* **32**, 4390 (1999).
41. M. Dalborg, K. Jacobson and S. Jonsson, *Polym. Degrad. Stabil.* **92**, 437 (2007).
42. C. Bell, P. Walker, M. Abeysondera, J. Simmons, P. King and G. Blunn, *J. Arthroplast.* **13**, 280 (2009).
43. O. K. Muratoglu, A. Mark, D. A. Vittetoe, W. H. Harris and H. E. Rubash, *J. Bone Joint Surg. Am.* **85**, S7 (2003).
44. B. M. Daly and J. Yin, *J. Biomed. Mater. Res.* **42**, 523 (1998).
45. R. J. Jacob, D. Pienkowski, K. Y. Lee, D. M. Hamilton, D. Schroeder and J. Higgins, *J. Biomed. Mater. Res.* **56**, 168 (2001).
46. S. Glyn-Jones, P. McLardy-Smith, H. S. Gill and D. W. Murray, *J. Bone Joint Surg. Br.* **90**, 556 (2008).
47. S. L. Bewill, G. R. Bevill, J. R. Penmetsa, A. J. Petrella and P. J. Rullkoetter, *J. Biomech.* **38**, 2365 (2005).
48. G. R. Plank, D. M. Estok II, O. K. Muratoglu, D. O. O'Connor, B. R. Burroughs and W. H. Harris, *J. Biomed. Mater. Res. Part B: Appl. Biomater.* **80**, 1 (2006).
49. F. J. Medel, C. M. Rinnac and S. M. Kurtz, *J. Biomed. Mater. Res. Part B: Appl. Biomater.* **89**, 530 (2008).
50. R. W. Hood, T. M. Wright and A. H. Burstein, *J. Biomed. Mater. Res.* **17**, 829 (1983).
51. F. J. Buchanan, J. R. White, B. Simand and S. Downes, *J. Mater. Sci. Mater. Med.* **12**, 29 (2001).
52. O. K. Muratoglu, C. R. Bragdon, D. O. O'Connor, M. Jasty and W. H. Harris, in: *Transactions of the 45th Annual Meeting, Orthopaedic Research Society*, February 1–4, Anaheim, CA, p. 817 (1999).
53. F. J. Buchanan, B. Simand and S. Downes, *Plastics Rubber Compd. Process. Appl.* **27**, 148 (1998).